

Investigation of the mechanical properties of a photocatalytic pseudo-paint

Afshin Dianatdar, Masoud Jamshidi

Polymer Research Laboratory, School of Chemical Engineering, Iran University of Science and Technology, Tehran, Iran

Correspondence to: M. Jamshidi (E-mail: mjamshidi@iust.ac.ir)

ABSTRACT: Photocatalytic oxidative paints (e.g., a paint containing nano-TiO₂) are used to break down volatile organic compounds to CO₂ by photooxidation reactions. In this research, a photocatalytic oxidative pseudo-paint was made with acrylic–styrene copolymer latex, TiO₂ pigment, calcium carbonate extender, and TiO₂ nanoparticles as a photocatalyst. To investigate the effects of the pigment, extender, and nanoparticles on the mechanical properties of the samples and their relationship to their photocatalytic activity, different contents of the particles were dispersed in the paint formulation. The tensile strengths (TSs) of the samples were measured as the mechanical properties. The samples were characterized by scanning electron microscopy analysis. We found that up to 3% nano-TiO₂ enhanced the mechanical properties of the pigmented resin, whereas beyond this, TS decreased. In samples containing 3% nanoparticles, the incorporation of 15% TiO₂ pigment caused optimized mechanical properties, and beyond that, TS decreased because of particle agglomeration. In the absence of nanoparticles, the samples showed improvements in the mechanical properties with up to a 40% loading of pigment. The results reveal that the samples containing nano-TiO₂ and pigment showed the same trend for the mechanical and photocatalytic properties before the critical pigment volume concentration (CPVC). However, when the extender was incorporated or TiO₂ particles were loaded beyond CPVC, the mechanical and photocatalytic properties correlation was compromised, and they were not directly correlated. © 2015 Wiley Periodicals, Inc. *J. Appl. Polym. Sci.* **2016**, *133*, 42885.

KEYWORDS: catalysts; coatings; composites; mechanical properties; microscopy

Received 14 May 2015; accepted 27 August 2015

DOI: 10.1002/app.42885

INTRODUCTION

Since the first report on the photocatalytic characteristics of TiO₂ in 1972, a lot of research has been devoted to using this potential to remediate indoor air pollution (mainly from volatile organic compounds and nitrogen oxides). Different operational parameters (humidity, temperature, load of nanocatalyst, light wavelength and intensity, residence time, type of contaminants, etc.) have been investigated thus far.^{1–3} Photocatalytic oxidation (PCO) needs the adsorption of contaminants on the surface of the nanocatalyst. Therefore, walls and ceilings, which are commonly covered by coatings and paints, tend to be suitable and huge surfaces on which PCO reactions can occur. On this basis, it makes sense to use photocatalytic paints as a wall coating to remove air pollution.

As the pioneers in this field, Fujishima and Honda (1972) discovered the phenomenon of photoinduced water cleavage to TiO₂ electrodes. Different studies have indicated that through the introduction of microsized particles (i.e., pigments and/or extenders) into paints, the characteristics of particles, such as the chemical nature, particle size, state of dispersion, morphol-

ogy, and loadings, determine the paint properties.⁴ The impact of the pigment on the modulus of elasticity, tensile strength (TS), and strain of organic coatings have been among the most investigated mechanical properties in the last 4 decades.^{4–7} For example, Li *et al.*⁸ studied the effect of TiO₂ nanoparticles on the TS of waterborne polyurethane (PU) and declared reinforcement of the binder by 0.25 wt % nanoparticle incorporation. This reinforcement was attributed to the homogeneous dispersion of nano-TiO₂ in the PU matrix and the interfacial interaction between nano-TiO₂ and PU. However, TS remained almost unchanged with increasing nanoparticle concentrations of up to 1 wt %. This was attributed to nanoparticle agglomeration. Cho *et al.*⁹ suggested that with decreasing particle size, the nanocomposite strength increased. They showed this phenomenon for both Young's modulus and TS. They concluded that a greater surface area provided more interfacial interactions and chain confinement. Liang *et al.*¹⁰ also prepared a nanocomposite, polyethylene containing polyacrylamide-grafted TiO₂, to achieve higher TSs.

Águia *et al.*¹¹ incorporated about 25% nano-TiO₂ into vinyl paint and showed that more than 80% of the nitric oxide could

be converted with that formulation. They also investigated the impact of a TiO₂ pigment and calcium carbonate (CaCO₃) extender and declared that pigmentary TiO₂ and nanoparticles absorbed the UV light competitively and that the TiO₂ pigment was the most critical component affecting the photocatalytic activity. On the other hand, extenders such as CaCO₃ impair the photoactivity. Monteiro *et al.*¹² incorporated 9 wt % (wet basis) TiO₂ nanoparticles into an exterior, water-based vinyl paint and obtained up to 90% conversion. Xiao *et al.*¹³ used acrylic–silicon films with 1% nano-TiO₂ and investigated the removal rate of formaldehyde and NO₂. They reported 76.7 and 68% removal of these gases, respectively. Gandolfo *et al.*¹⁴ investigated NO₂ conversion via the incorporation of 0–7% nano-TiO₂ into an already available photocatalytic paint and reported that the uptake coefficients of the paints toward NO₂ increased from 5×10^{-6} to 1.6×10^{-5} .

The topic of photocatalytic paint is still under investigation and optimization. However, to our knowledge, there have been few studies on the mechanical properties of such paints, so this itself could be a challenge. As mentioned, sometimes a high percentage of nanoparticles have been used in a paint to obtain a higher PCO performance; on the other hand, binder photodegradation as a result of PCO activity should also be addressed.^{15–19} Therefore, the assessment of the mechanical properties of photocatalytic paint as representative of material degradation could be investigated.

The dispersion of nanoparticles in polymers and their impact on the mechanical properties, including TS, stiffness, and elongation at break, have been determined previously.^{20,21}

In this research, the effect of using nanosized TiO₂ along with microsized TiO₂ as a pigment and CaCO₃ as an extender on the mechanical properties and PCO rate of an acrylic–styrene water-based polymer were investigated. For this purpose, samples with different contents of nanoparticles were prepared, and TS of the samples were measured. In the next step, different contents of TiO₂ pigment were added to nano-TiO₂-containing polymer composites. The optimum content of pigment in the presence of nanoparticles was determined. After that, CaCO₃ was added to the polymer (i.e., with and without nanoparticles and pigment). The tensile behavior of all of the samples were measured. The dispersion of the particles in the polymer matrix was analyzed through scanning electron microscopy (SEM) analysis. Finally, photocatalytic tests for the selected films were performed. The mechanical properties and photocatalytic performance of the nanocomposite pseudo-paints were evaluated through different loadings of paint components.

EXPERIMENTAL

Materials

Acrylic–styrene copolymers (R-4410 and NS-87) were used as the resin; these were produced by Simab Resin Co. R-4410 (minimum film formation temperature = 20°) was mixed with NS-87 (minimum film formation temperature = 8°) with a ratio of 3:1, and the mixture was used as the final resin. Both were anionic with pHs between 8 and 10. Kronos-2190 was used as pigmentary TiO₂. CaCO₃ was purchased from Polymer Concrete

Co. and was used as the extender. Nano-TiO₂ (Tecnan Co., particle size = 10–15 nm) was used as the nanocatalyst. Poly(acrylic acid) (molecular weight = 20,000 g/mol) was used as the dispersant. Benzene was purchased from Merck Co. and was used as a volatile organic compound. A PU-based thickener and commercially available antifoam were used as additives to make defect-free films.

Photocatalytic Paint Production

At first, poly(acrylic acid) was dispersed in deionized water with an ultrasonic homogenizer (i.e., Bandelin 3200), and the pH was adjusted to 11 through the addition of NaOH. Pigmentary TiO₂ was then sonicated in an aqueous dispersant with a 10:1 ratio. Likewise, nano-TiO₂ was sonicated at a ratio of 4:1. CaCO₃ was milled in a planetary mill with a power of 200 W for 1 h. Finally, all components of the mixture were sonicated for 15 min with a power of 30 W and a pulse of 1 s. The sample pH was adjusted to 10. All of the formulations are presented in Table I.

After sonication, the mixture was slowly stirred, and then, the antifoam and thickener were added. Then, with a film applicator, a 200- μ m wet film for the photocatalytic samples and a 400- μ m wet film for tensile tests were applied on a polyethylene slab. The films were placed in an oven at 60°C for 3 h, and curing was continued in ambient environment for 24 h in a dark chamber.

Mechanical Properties

To investigate the mechanical properties of the samples, a Santam 150 universal machine was used. ASTM D 2370²² was followed for specimen preparation and test methods. Ten test specimens were prepared from each film sample, and their tensile behaviors were evaluated. Then, according to the calculation procedure of the standard, the TS, elongation at break, and modulus of elasticity were calculated on the basis of eqs. (1–3), respectively. Finally, the area under the stress–strain curve was calculated as the fracture toughness.

To determine the particle dispersion and its impact on the mechanical properties, SEM was used (Hitachi S4160).

$$TS = \frac{P_R}{TW} \quad (1)$$

$$E = 100 \frac{\Delta L}{L} \quad (2)$$

$$S = \frac{P_E}{TW} \quad (3)$$

where ΔL is the increase in the specimen length to break (mm), L is the initial specimen length (mm), P_R is the tensile pull to rupture (N), T is the thickness of the test specimen (mm), W is the width of the test specimen (mm), P_E is the load force (N) to elongate the film 1% from the first point in the stress–strain curve where the slope remains constant, E is the elongation at break, and S is the modulus of elasticity (stiffness).

PCO Analysis

After the samples were prepared, they were put on a glass slab inside the photocatalytic test chamber.²³ The benzene vapor was injected into the chamber, and air circulation via fans was

Table I. Formulations of the Photocatalytic Films

Sample code	Nanocatalyst: Nano-TiO ₂ (%)	Pigment: TiO ₂ (%)	Extender: CaCO ₃ (%)	Additives (%)	PVC ^a
Control	—	—	—	1	—
N1	1	—	—	1	0.284
N3	3	—	—	2	0.87
N5	5	—	—	2	1.46
T15	—	15	—	2	4.9
T25	—	25	—	2	8.2
T30	—	30	—	2	11.4
T40	—	40	—	2	17.6
T15-N3	3	15	—	2	5.6
T25-N3	3	25	—	2	9.1
T30-N3	3	30	—	2	12.1
T40-N3	3	40	—	2	18.2
T15-N5	5	25	—	2	6.1
C	—	—	8	1	4.1
C8-N3	3	—	8	1	5
PsP (T15-N3-C)	3	15	8	2	9.4

^a PVC $\frac{V_{\text{pigment}} + V_{\text{extender}} + V_{\text{nanoparticles}}}{V_{\text{pigment}} + V_{\text{extender}} + V_{\text{nanoparticles}} + V_{\text{nonvolatiles}}}$, where V is the volume of the respective materials.
PsP Pseudo-Paint.

started. The system was left for 5 h to come to a steady state. The conditions of the test chamber remained constant during the tests. The PCO analysis was performed on different samples. The samples examined for PCO performance are listed in Table II.

RESULTS AND DISCUSSION

Effect of Sonication on the Polymer Properties

It has long been known that when polymers are sonicated, high-molecular-weight polymer chains may break into lower molecular weight chains because of shear forces. This phenomenon is also known as the chain scission of polymers and/or polymer degradation, which happens as a result of the high energy of sonication.^{24–26} Therefore, as a result of latex sonication, the mechanical properties can change. Figure 1 demonstrates stress–strain curves for the pure latex films (i.e., control samples) with and without sonication.

As shown, through sonication of latex, both the ultimate strength and extensibility of the samples decreased. In this

research, the C-S15 sample (i.e., the pure latex sample, which experienced 15 min sonication) was selected as the control sample. The results for this sample were compared to the ones of the nanocomposite paints. This was because we used 15 min of sonication during the paint preparation process.

Effect of the TiO₂ Nanoparticles

Figure 2 shows the TSs of the acrylic–styrene copolymer containing different amounts of nano-TiO₂. It is well known that when the amount of reinforcing particles into latex film is increased, TS increases when there is good dispersion and interaction between the polymer and particles.⁴ It was evident that TS of the control sample was improved more than 100% when up to 3% nanoparticles were incorporated. However, when the nanoparticle content was increased up to 5%, TS decreased. This was attributed to the reagglomeration of nano-TiO₂ in the matrix.²⁷

SEM analysis was used to assess the dispersion of nano-TiO₂ in these samples. Figure 3(a) shows the smooth cross section of the control sample. Figure 3(b) shows the agglomeration of

Table II. Samples Examined for the PCO Rate

Run	Sample code
1	N3
2	N5
3	T15-N3
4	T25-N3
5	T30-N3
6	T40-N3
7	PsP (i.e., T15-N3-C)

PsP Pseudo-Paint.

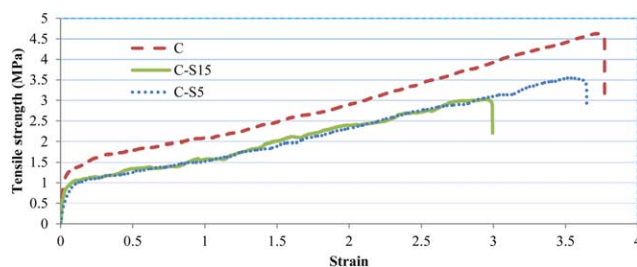


Figure 1. Variation in the stress–strain behavior for the resin without sonication (C), the resin with 5 min of sonication (C-S5), and the resin with 15 min of sonication (C-S15). [Color figure can be viewed in the online issue, which is available at wileyonlinelibrary.com.]

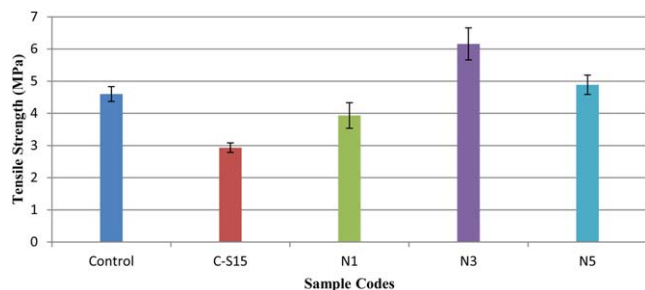


Figure 2. TSs of the acrylic-styrene copolymer nanocomposites. [Color figure can be viewed in the online issue, which is available at wileyonlinelibrary.com.]

nano-TiO₂ particles with sizes bigger than 2 μm. This image confirmed the reagglomeration of nano-TiO₂ at 5% incorporation into the latex.

Effect of the TiO₂ Pigment

The effect of the TiO₂ pigment on the tensile behavior of the nanocomposite was investigated. Figure 4 illustrates the effects of different amounts of TiO₂ pigments on the TS of a nanocomposite containing 3% nano-TiO₂.

It was obvious that when the TiO₂ content was increased, TS decreased. Also, a concentration of 15% TiO₂ increased TS up to 50%. This behavior was attributed to the wetting capability of

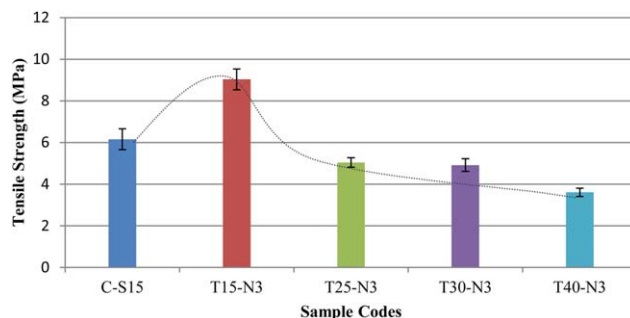


Figure 4. TSs of nanocomposites containing different amounts of TiO₂ pigment. [Color figure can be viewed in the online issue, which is available at wileyonlinelibrary.com.]

the solid particles by latex. It was obvious that the latex could not wet a large number of particles, as they introduced air pockets into the sample. This porosity caused local stress concentration and decreased TS. To better understand this, we performed SEM analysis. The results are shown in Figure 5. As shown in Figure 5(a), the particle dispersion in the T15-N3 sample was very good, but when the pigment content was increased up to 40%, as illustrated in Figure 5(b–d), agglomerates started to grow.

To elucidate the role of nanoparticle on the load-bearing capacity of the samples, the same samples were also prepared in the absence of nanoparticles. The TS test results are demonstrated in Figure 6. It was clear that with no nanocatalyst in the formulation, TS improved even up to a 40% incorporation of pigment. This showed how the existence of nanoparticles restricted the matrix loading capacity of the particles, a fact that should be taken into account during the preparation of a photocatalytic paint. This was attributed to the very high surface area of nano-TiO₂, which eliminated the contribution of latex in the wetting of the TiO₂ pigments.

To evaluate the simultaneous effect of nanoparticles and TiO₂ pigments, samples were prepared at constant amount of pigment (i.e., 15%) with different amounts of nano-TiO₂. Figure 7 shows the results. Again, it could be inferred that an increase in the nanoparticle content up to 5% decreased TS; this confirmed our previous conclusion about the fall in the strength of the samples due to weak dispersion. It was obvious that the use of nano-TiO₂ had a positive effect on the presence of the 15% TiO₂ pigment.

The elastic modulus of the samples was also determined. The results are shown in Figure 8(a–d). The modulus of elasticity was used to find the critical pigment volume concentration (CPVC) because it increased up to CPVC and decreased after that because of air pocket intrusion into the binder.^{15,28}

Figure 8(a) shows how the addition of nano-TiO₂ increased the rigidity of the film. It also suggests that at nanoparticle contents greater than 3%, the stiffness did not increase any further. This implied agglomeration of the nanoparticles. Figure 8(b) suggests that in the presence of 3% nanoparticles in the binder, about 25% pigment could be added to the mixture before CPVC was surpassed. Figure 8(c), however, implies that when there were no nanoparticles in the formulation, up to 40% pigment could

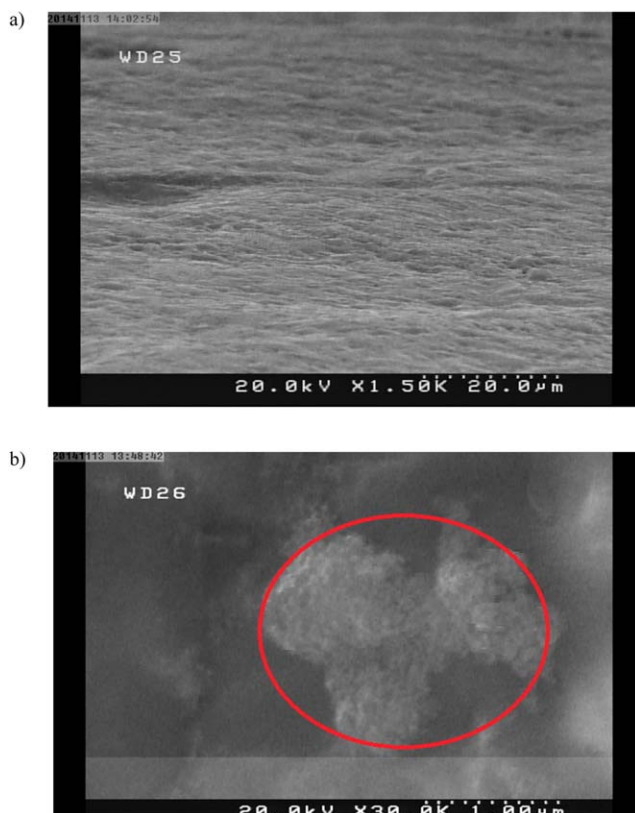


Figure 3. SEM micrographs of the (a) a control sample and (b) N5 (the circle shows the agglomerate size of approximately 2 μm). [Color figure can be viewed in the online issue, which is available at wileyonlinelibrary.com.]

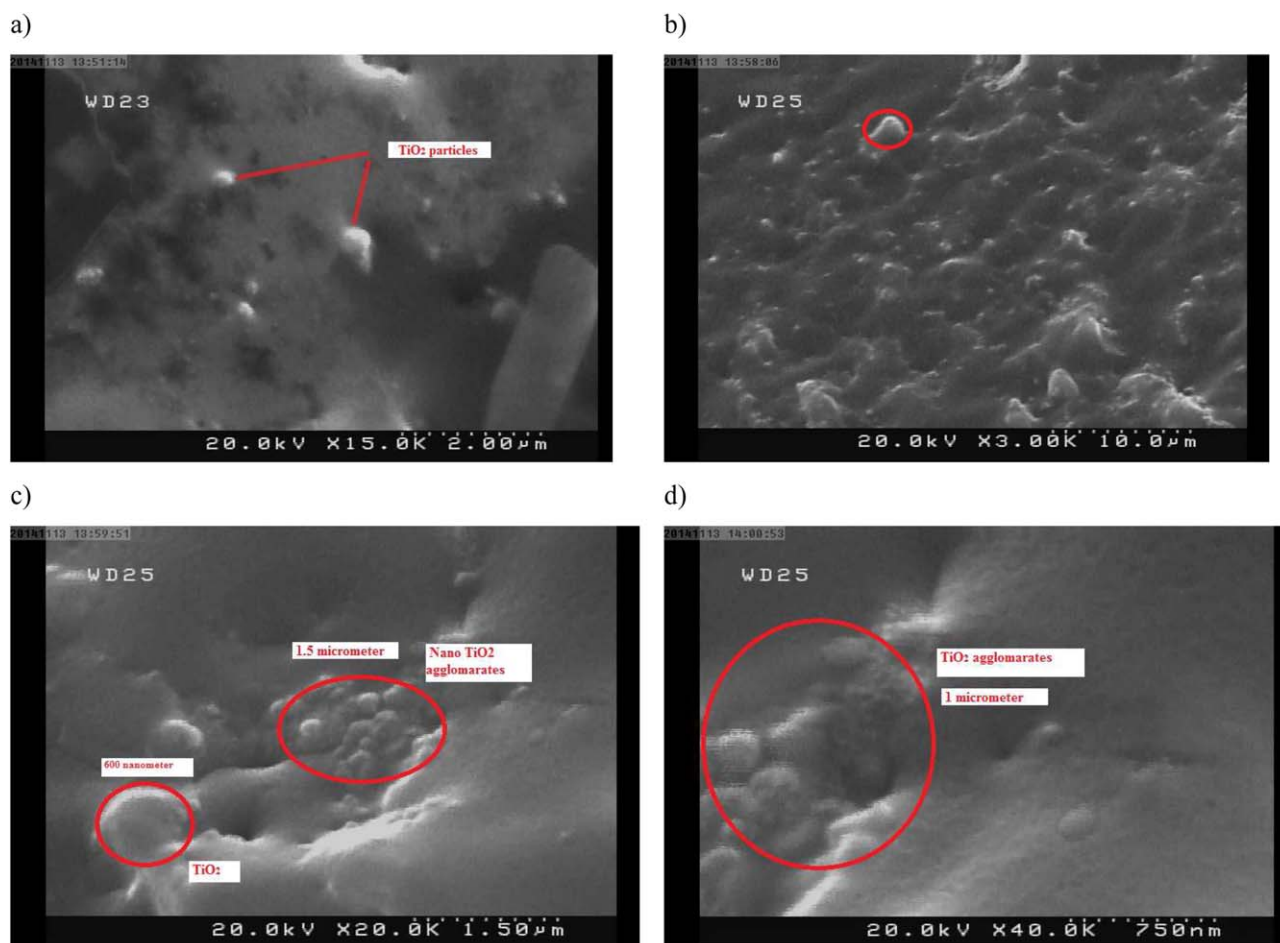


Figure 5. SEM micrographs of the cross sections of the samples: (a) T15-N3, (b) T25-N3, (c) T30-N3, and (d) T40-N3. [Color figure can be viewed in the online issue, which is available at wileyonlinelibrary.com.]

be dispersed without any negative effect on the polymer stiffness. However, the maximum stiffness obtained in this case was too much lower (i.e., one-third) than when nano-TiO₂ and micro-TiO₂ were used together in the formulation. Figure 8(d) suggests that with 15% TiO₂ in the binder, the addition of more than 3% nano-TiO₂ caused the stiffness to decline. An interesting point was that when nanoparticles were used in the formulation, the value of the pigment volume concentration (PVC) was not so representative. This indicated that despite the low values of the PVCs (e.g., 1.46 and 5.6 for N5 and T25-N3, respectively), the

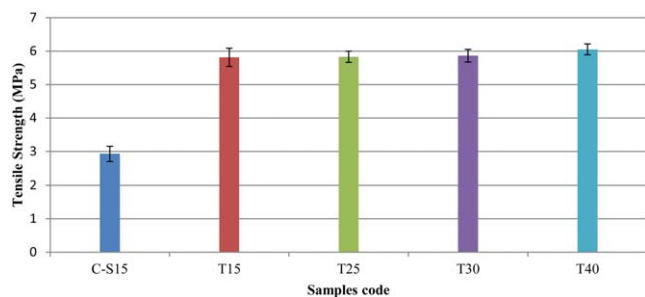


Figure 6. TSs of acrylic-styrenes containing different amounts of TiO₂ pigment. [Color figure can be viewed in the online issue, which is available at wileyonlinelibrary.com.]

films showed weak performances, such as when the samples surpassed CPVC. This was attributed to the existence of nanoparticles in the formulation. This was attributed to the fact that the nanoparticles restricted pigment wetting.

The results of the elongation at break are presented in Figure 9. Figure 9(a-d) shows that an increase in the nanoparticle content to 5% showed similar results to an increase in the pigment content up to 40%. The interesting point was the intensity to which elongation at break decreased.

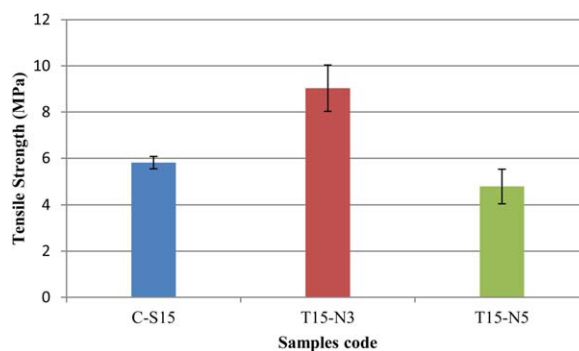


Figure 7. TSs of samples containing 15% TiO₂ and different amounts of nanoparticles. [Color figure can be viewed in the online issue, which is available at wileyonlinelibrary.com.]

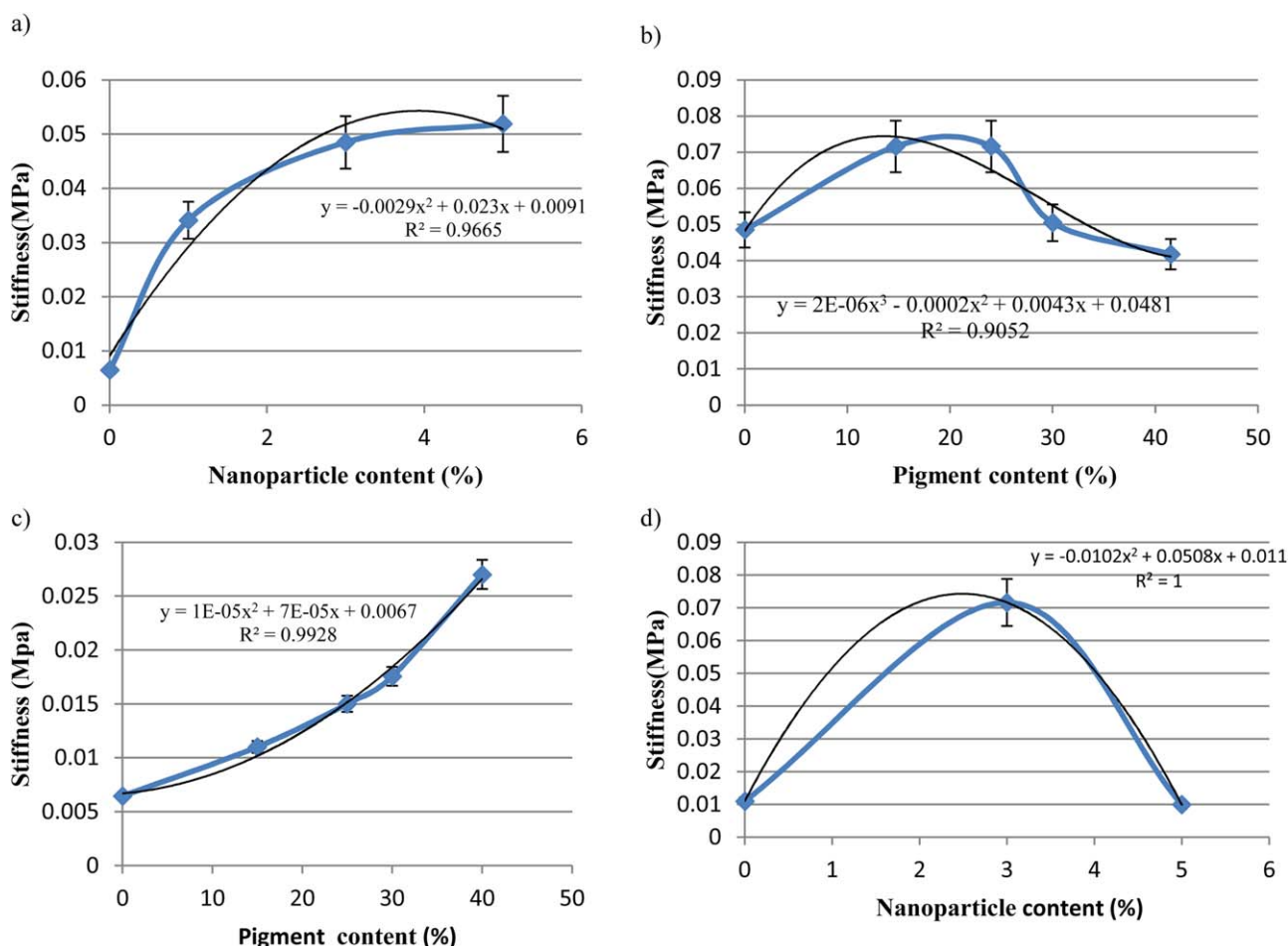


Figure 8. Modulus of elasticity values of the samples containing (a) nanoparticles, (b) 3% nano-TiO₂ and different amounts of TiO₂ pigment, (c) TiO₂ pigment, and (d) 15% TiO₂ pigment and different amounts of nano-TiO₂. [Color figure can be viewed in the online issue, which is available at wileyonlinelibrary.com.]

Figure 9(a–c) suggests that the impact of 3% nanoparticles was somehow similar to the effect of 30%–40% microsized TiO₂ in decreasing the elongation of the samples. A comparison of Figure 9(b) with Figure 9(c) shows how the existence of nanoparticles intensified the impact of the TiO₂ pigments when the elongation decreased. It was evident that the existence of 3% nano-TiO₂ along with 15% TiO₂ caused a fall of 2.5 times in the elongation at break; this also indicated an increase in the stiffness of the samples.

The results of the toughness are illustrated in Figure 10(a–d). As demonstrated in Figure 10(a,d), the increase in the nanoparticle content decreased the toughness. On the other hand, Figure 10(b,c) suggests that the toughness increased up to a 25% loading of pigment and, after that, decreased. This was attributed to the fact that at lower solid contents, the polymer films were more flexible, but with greater solid contents, they tended to become rigid.

Effect of the Extender

To assess the mechanical performance of the pseudo-paint, CaCO₃ was added to the formulation, including latex, pigment, and nanoparticles. The mechanical properties of the sample

were measured in a manner similar to those of the previous samples. The results are shown in Table III. The addition of CaCO₃ to the binder (i.e., C8 sample) improved TS by about 50%, but when we involved pigment and nanoparticles in the formulation (i.e., Pseudo-Paint (PsP) sample), the mechanical properties did not increase significantly. This was attributed to the high solid content of the Pseudo-Paint (PsP) sample, which increased sample porosity. It is well known that latex has a limited capability of solid particle wetting because of the fact that most water-based paints are made with moderate solid contents; nevertheless, the solids sedimented.

PCO Test

Table IV presents the PCO test results. We discussed before how the addition of greater than 3% nanoparticles decreased the mechanical properties because of poor dispersion. This fact happened to be the reason why PCO of benzene fell around 50% in the sample containing 5% nano-TiO₂ (i.e., N5 sample) in comparison to the N3 sample. The effects of the TiO₂ pigment and CaCO₃ extender were both beneficial. TiO₂ and CaCO₃ made the films more porous, so they eased contaminant diffusion into film and on the catalyst sites. Unlike the mechanical properties, up to 40% pigment loading had a positive impact on

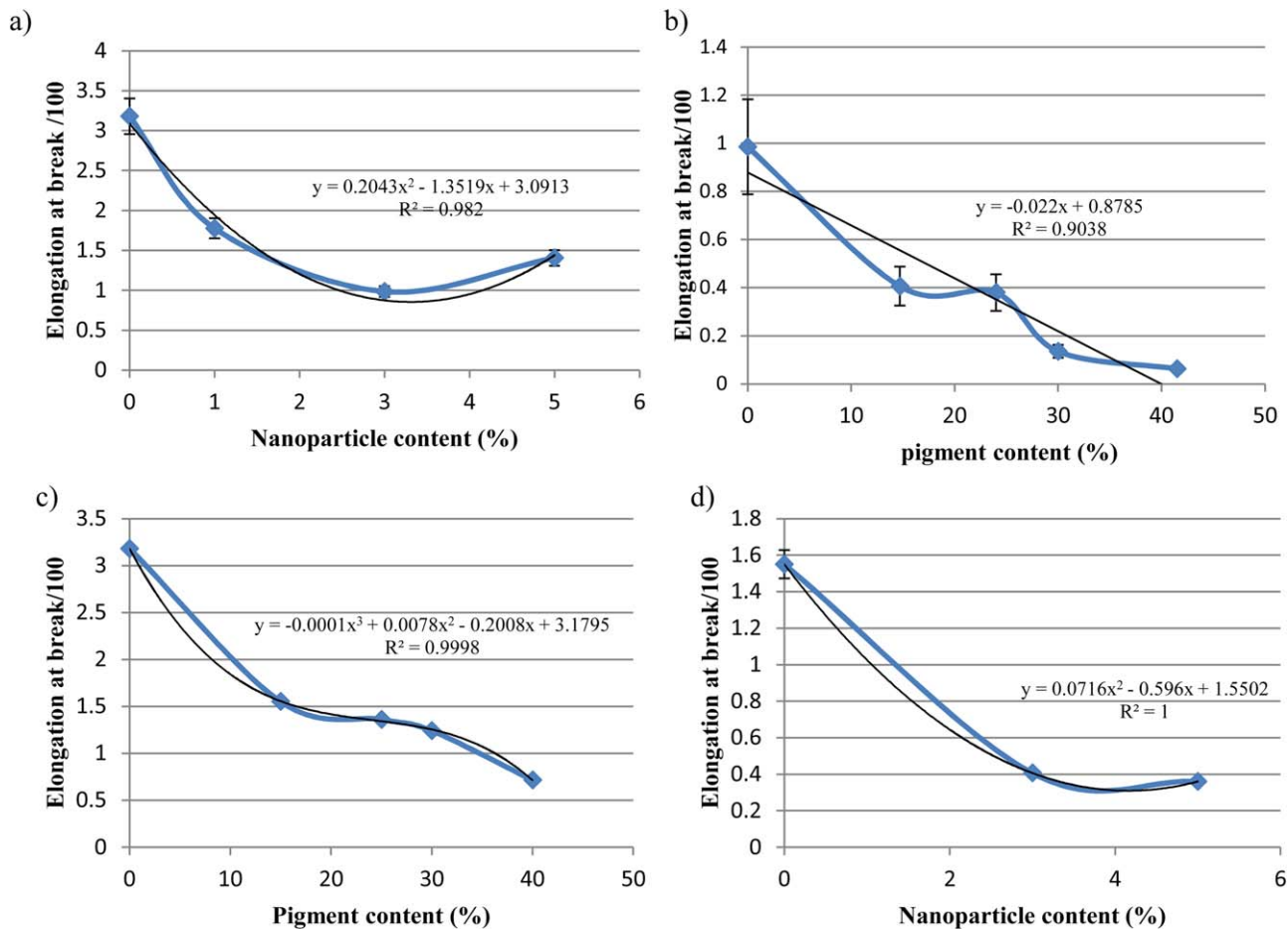


Figure 9. Elongation at break of the samples containing (a) nanoparticles, (b) 3% nano-TiO₂ and different amounts of TiO₂ pigment, (c) TiO₂ pigment, and (d) 15% TiO₂ pigment and different amounts of nano-TiO₂. [Color figure can be viewed in the online issue, which is available at wileyonlinelibrary.com.]

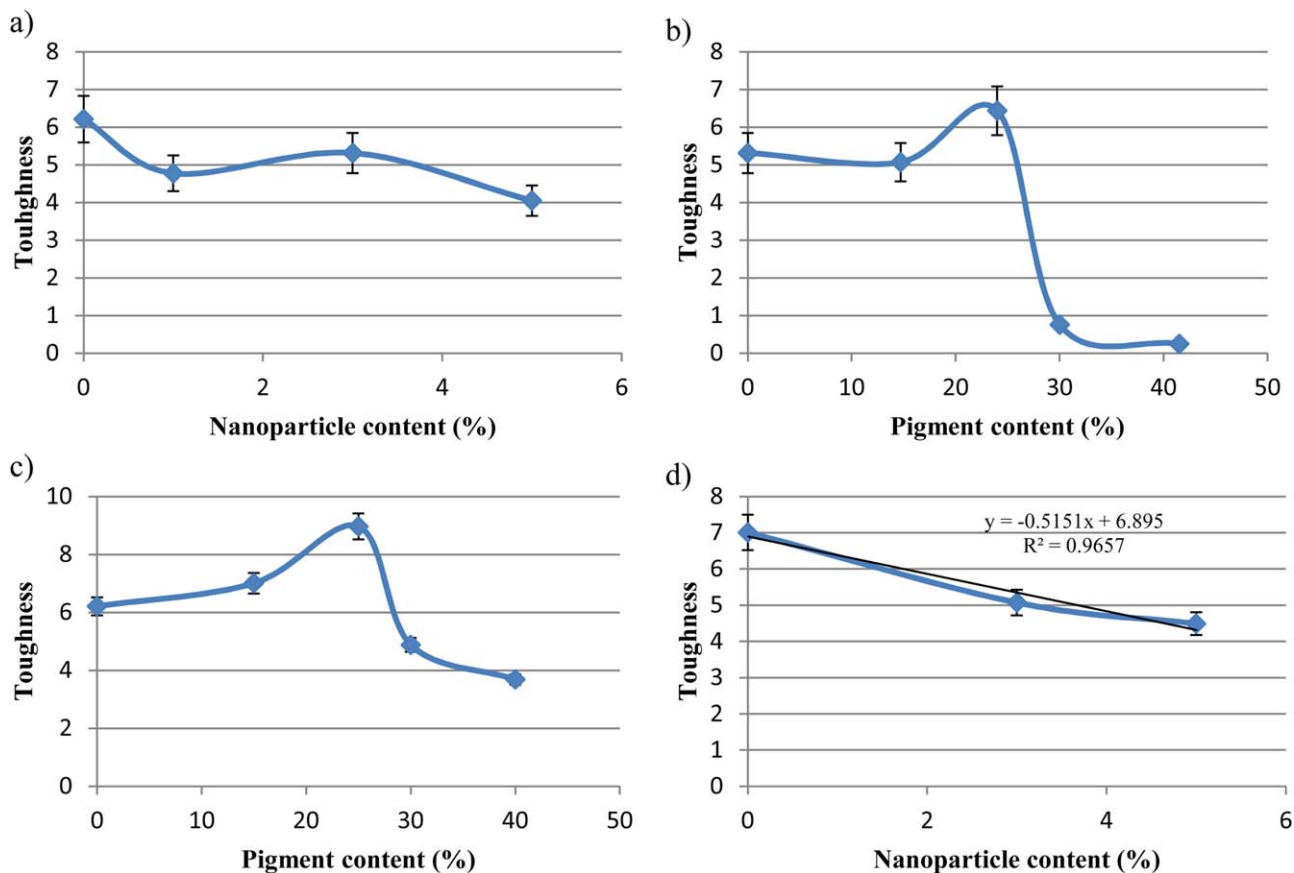


Figure 10. Fracture toughness of the samples containing (a) nanoparticles, (b) 3% nano-TiO₂ and different amounts of TiO₂ pigment, (c) TiO₂ pigment, and (d) 15% TiO₂ pigment and different amounts of nano-TiO₂. [Color figure can be viewed in the online issue, which is available at wileyonlinelibrary.com.]

Table III. Variation of the Mechanical Properties through the Incorporation of CaCO₃

Sample code	TS ^a (MPa)	Standard deviation	Elongation at break (%)	Standard deviation	Stiffness (MPa)	Standard deviation	Toughness (N m)	Standard deviation
Control	2.93	0.22	3.18	0.42	0.0064	0.00199	6.21	0.37
C8	4.23	0.21	1.096	0.12	0.0113	0.0027	3.21	0.50
T15-N3	9.032	0.52	0.38	0.0368	0.0715	0.0057	5.06	0.51
PsP (T15-N3-C)	4.41	0.26	1.66	0.274	0.0132	0.0005	5.42	1.101

^aTS, Tensile Strength.

Table IV. Photocatalytic Properties of the Selected Photocatalytic Coatings

Sample code	Benzene removal ($\mu\text{g cm}^{-2} \text{h}^{-1}$)
N3	0.31
N5	0.17
T15-N3	0.35
T25-N3	0.70
T30-N3	1.66
T40-N3	0.44
PsP (T15-N3-C)	1.1

PCO. TiO₂ may have enhanced light absorption and scattering and so could be a favorite for photocatalytic reaction occurrence. The use of CaCO₃ in the presence of 15% pigment showed a synergistic influence on increasing the PCO performance in the samples.

CONCLUSIONS

Photocatalytic pseudo-paint was prepared with a water-based acrylic-styrene copolymer, TiO₂ pigment, CaCO₃ extender, and nano-TiO₂. The mechanical properties and photocatalytic performance of the samples were evaluated. Our conclusions follow:

1. The incorporation of nanoparticles had a negligible effect on the PCO activity but improved the mechanical performance of the latex films, especially when the nanoparticles were not agglomerated.
2. The addition of TiO₂ pigment increased TS and stiffness; however, in the presence of nanoparticles, there was a limitation for wetting the pigment with binder. This caused a decrease in the mechanical properties.
3. The addition of CaCO₃ as an extender improved the mechanical properties of the pure acrylic-styrene sample. However, in the presence of TiO₂ particles, it did not show a significant impact on the properties.
4. The presence of TiO₂ pigment was found to be necessary for PCO activity, and when the TiO₂ content was increased by two times, PCO activity increased four times.
5. The addition of CaCO₃ showed an increase in the PCO activity of up to three times.

REFERENCES

1. Wang, S.; Ang, H. M.; Tade, M. O. *Environ. Int.* **2007**, *33*, 694.
2. Mo, J.; Zhang, Y.; Xu, Q.; Lamson, J. J.; Zhao, R. *Atmos. Environ.* **2009**, *43*, 2229.
3. Chen, J.; Poon, C. *Build. Environ.* **2009**, *44*, 1899.
4. Perera, D. Y. *Prog. Org. Coat.* **2004**, *50*, 247.
5. Schrager, M. J. *Appl. Polym. Sci.* **1978**, *22*, 2379.
6. Manson, J. A.; Sperling, L. H. *Polymer Blends and Composites*; Plenum: New York, **1976**.
7. Ikeda, S. *Prog. Org. Coat.* **1973**, *1*, 205.
8. Li, K.; Peng, J.; Zhang, M.; Heng, J.; Li, D.; Mu, C. *Colloid Surf. A* **2015**, *470*, 92.
9. Cho, J.; Joshi, M. S.; Sun, C. T. *Compos. Sci. Technol.* **2006**, *66*, 1941.
10. Liang, W.; Luo, Y.; Song, S.; Dong, X.; Yu, X. *Polym. Degrad. Stab.* **2013**, *98*, 1754.
11. Águia, C.; Ângelo, J.; Madeira, L. M.; Mendes, A. *Catal. Today* **2010**, *151*, 77.
12. Monteiro, R. A. R.; Lopes, F. V. S.; Silva, A. M. T.; Ângelo, J.; Silvad, G. V.; Mendes, A. M.; Boaventura, R. A. R.; Vilar, V. J. P. *Appl. Catal. B* **2014**, *147*, 988.
13. Xiao, G.; Huang, A.; Su, H.; Tan, T. *Build. Environ.* **2013**, *65*, 215.
14. Gandolfo, A.; Bartolomei, V.; Alvarez, E. G.; Tlili, S.; Gligorovski, S.; Kleffmann, J.; Wortham, H. *Appl. Catal. B* **2015**, *166*, 84.
15. Allen, N. S.; Edge, M.; Ortega, A.; Sandoval, G.; Liauw, C. M.; Verran, J.; Stratton, J.; McIntyre, R. B. *Polym. Degrad. Stab.* **2004**, *85*, 927.
16. Miyazaki, K.; Arai, T.; Nakatani, H. *J. Appl. Polym. Sci.* **2014**, *131*, 39909.
17. Yang, C.; Tian, L.; Ye, L.; Peng, T.; Deng, K.; Zan, L. *J. Appl. Polym. Sci.* **2011**, *120*, 2048.
18. Nakatani, H.; Miyazaki, K. *J. Appl. Polym. Sci.* **2013**, *129*, 3490.
19. Miyazaki, K.; Sato, H.; Kikuchi, S.; Nakatani, H. *J. Appl. Polym. Sci.* **2014**, *131*, 9205.
20. Singh, S. K.; Tambe, S. P.; Kumar, D. J. *Mater. Sci.* **2004**, *39*, 2629.
21. Toussaint, A. *Prog. Org. Coat.* **1973**, *2*, 237.
22. American Society for Testing and Materials. Standard Test Method for Tensile Properties of Organic Coatings; ASTM

- D 2370; American Society for Testing and Materials: West Conshohocken, PA, **2010**.
23. Dianatdar, A.; Jamshidi, M. M.S. thesis, Iran University of Science and Technology, **2014** (in Persian).
24. Koda, S.; Taguchi, K.; Futamura, K. *Ultrason. Sonochem.* **2011**, *18*, 276.
25. Konaganti, V. K.; Madras, G. *Ultrason. Sonochem.* **2010**, *17*, 403.
26. Mohod, A. V.; Gogate, P. R. *Ultrason. Sonochem.* **2011**, *18*, 727.
27. Fasaki, I.; Siamos, K.; Arin, M.; Lommens, P.; Driessche, I. V.; Hopkins, S. C.; Glowacki, B. A.; Arabatzis, I. *Appl. Catal. A* **2012**, *411*, 60.
28. Mirabedini, S. M.; Kiamanesh, A. *Prog. Org. Coat.* **2013**, *76*, 1625.